Preprint
UCRL-JC-153762

Investigation of Main-Chamber and Divertor Recycling in DIII-D Using Tangentially Viewing CID Cameras

M. Groth, G. D. Porter, T. W. Petrie, M. E. Fenstermacher, N. H. Brooks

This article was submitted to: *30th EPS Conference on Controlled Fusion and Plasma Physics, St Petersburg, Russia 7/07/2003 – 7/11/2003*

June 16, 2003

U.S. Department of Energy
Lawrence Livermore National Laboratory

This work was performed under the auspices of the United States Department of Energy by the University of California, Lawrence Livermore National Laboratory under contract No. W-7405-Eng-48.

Investigation of Main-Chamber and Divertor recycling in DIII-D Using Tangentially Viewing CID Cameras

M. Groth,[1] G.D. Porter,[1] T.W. Petrie,[2] M.E. Fenstermacher,[1] and N.H. Brooks[2]

[1] *Lawrence Livermore National Laboratory, P.O. Box 808, Livermore, California 94550 USA*

[2] *General Atomics, P.O. box 85608, San Diego, California 92186 USA*

Abstract. Measurements of the D_α emission profiles from the divertor and main chamber region in DIII-D, performed in low-density L-mode, and low and high-density ELMy H-mode plasmas imply that core plasma fueling occurs through the divertor channel. Emission profiles of carbon, combined with UEDGE modeling of the L-mode plasmas, also suggests that chemical sputtering of carbon from the flux surface adjacent to the inner divertor walls, and temperature gradient forces in the scrape-off layer, determine the carbon content of the inner main chamber scrape-off layer.

1. Introduction and principal diagnostics

Significant main-chamber recycling in tokamaks has detrimental effects on plasma performance and particle control, and draws serious implications for the design of future fusion reactors. Main-chamber recycling enhances the sputtering of material from the main walls due to plasma contact, and elevated charge-exchange resulting from a larger neutral density in the main chamber, which in turn diminishes the ability to restrict plasma-surface interactions to the divertor region. Regimes that exhibit significant fractions of main-chamber recycling to the total core plasma fueling and impurity content have been reported from other fusion experiments [1,2].

To assess the role of main-chamber recycling in DIII-D, tangentially viewing charge-injected device (CID) cameras examining the divertor and main-chamber regions in the visible wavelength range were employed [3,4]. Mounted at different toroidal locations, the viewing geometry of each camera projected onto a poloidal plane (Fig. 1). A midplane camera system was added to DIII-D during the 2002 experimental campaign to measure inner and outer wall emission profiles in a region ±0.6 m vertically around the tokamak midplane. Light collected through a wide-angle mini lens (FOV 40°) was relayed via a fiber image guide, and through a set of neutral density and interference filters, to an intensified CID camera. Line-integrated emission profiles of the inner scrape-off layer (SOL) were obtained at the D_α (656.3 nm), carbon-II (515.1 nm), and carbon-III 464.7 nm) transitions, and their poloidal distribution profile calculated using Abel inversion and tomographic reconstruction techniques [3].

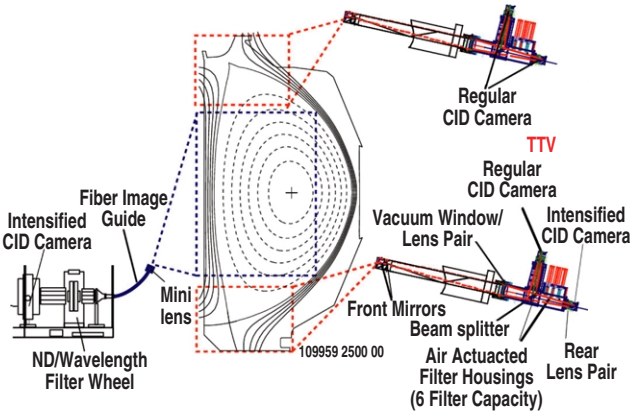

Fig. 1. Viewing geometry of the DIII-D tangential camera system superimposed on the DIII-D vacuum vessel and a double-null, high-triangular magnetic configuration. Size of the camera system is exaggerated for illustration purpose.

3. Recycling in Low-Density L-Mode Discharges

Detailed analysis of main-chamber recycling in DIII-D was performed for low-density (n/n_{GW}~0.2), low-confinement plasmas, which were specifically designed to characterize the main and divertor SOL plasma [5].

The measured D_α and CII emission profiles in the lower divertor indicated a well-attached divertor plasma, and variation in the emission between the inner and outer divertor leg. Both emission profiles peaked at the material surfaces, and the D_α emission partially extended upstream along the inner divertor leg. The D_α emissivity was about twice as high at the inner strike point as at the outer. In contrast, CII emission was about three times higher at the outer strike point than at the inner.

Tomographic reconstructions of the D_α, CII, and CIII emission profiles measured by the midplane camera show the D_α emission dominant in the vicinity of the X-point inside the separatrix [Fig.2(a)], whereas the carbon emission regions were observed outside the main plasma, peaking at the bottom part of the camera view, and extending further upstream with the charge state of the carbon ion [Fig. 2(b-c)]. Characteristically, the D_α emission at the lower boundary of the camera view was about three orders of magnitude smaller than at the divertor plate. Emission from the outer wall region was within the background noise.

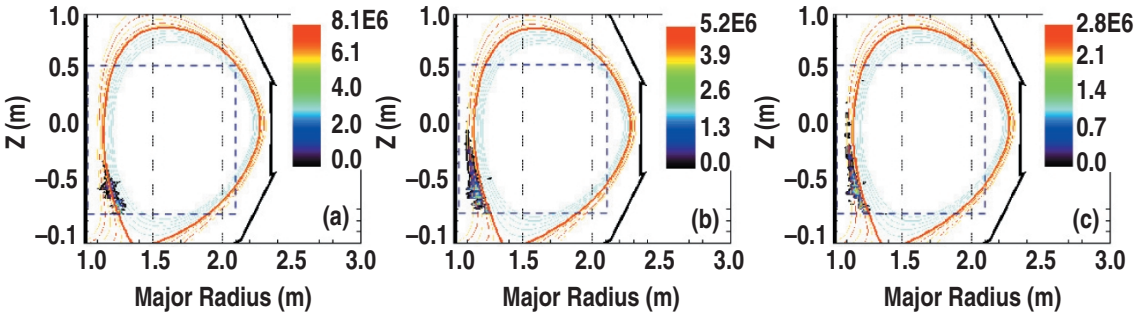

Fig. 2. Tomographic reconstruction of the D_α (a), CII (b), and CIII (c) poloidal emission profiles for low-density L-mode plasmas. The camera field-of-view is visualized by the rectangle, which is also the region tomographically reconstructed. Intensities are given in arbitrary units.

The 2-D edge fluid code UEDGE [6] was employed to simulate the SOL of these L-mode plasmas, and the solutions were benchmarked against the Thompson scattering and a system of downward viewing photo-multiplier arrays. The simulations included the effect of plasma **E×B** and **B×∇B** drifts, and the effect of carbon impurity created by physical and chemical sputtering [7,8]. A multi-ion impurity model was used in which the density of each charge state is determined using a parallel force balance for transport along the magnetic field. Radial transport of the fuel and impurity ions was assumed anomalous, and was modeled with spatially constant coefficients for the particles ($D_\perp$ = 0.2 m^2/s), and electron and ion thermal transport ($\chi_\perp$=0.8 m^2/s). These coefficients were obtained by fitting the simulated radial profiles of the plasma density and temperature near the midplane to those obtained experimentally by Thompson scattering. Simulated data of the photo-multiplier array at D_α, D_γ, and CIII at 464.7 nm agree with the experiment to within a factor of two. Qualitatively, the UEDGE calculated 2-D poloidal D_α and CII emission profiles in the divertor capture most of the features as measured by the divertor tangential camera.

Above the divertor region, the simulated emission profiles for D_α, CII, and CIII are in agreement with the experimental data, and imply plasma fueling through the divertor X-point and main SOL carbon arising from chemical sputtering from the divertor walls. The modeled D_α profile is strongly dominated by emission from the divertor and X-point region, and is found both outside and inside the separatrix, in agreement with the data. Since deuterium radiates as a neutral only, this implies that the divertor X-point region is the source of fueling of the core plasma from recycling neutrals. The poloidal extent of the modeled CII and CIII emission is significantly greater than that of deuterium, and the emissivity of both species peaks well outside the main plasma. Despite much larger carbon sources arising from physical and chemical sputtering from the ion and neutral fluxes to the target plates, the net deposition of carbon to the plates results from chemical sputtering from the outer flux surface of the divertor walls and, to some lesser extent, the private flux. The carbon sputtered off the plates is essentially re-ionized immediately, and re-deposits on the same plate. On the high-field side the carbon source of the divertor wall extends up to 20 cm off the inner plate, with very small contribution beyond it. A balance between the ion temperature gradient force and a somewhat weaker friction force due to collisions with the background plasma transports the C^{+1} ions away from the divertor, and they continue to radiate as the carbon is ionized to higher ionization stages. Consistent with this model, the observed CIII emissivity extended much further poloidally than CII.

4. Recycling in Low and Medium-Density ELMy H-Mode Discharges

Main-chamber recycling was experimentally investigated in low (n/n_{GW}~0.4) and medium (n/n_{GW}~0.6) density, high-confinement discharges with type-I edge-localized modes (ELMs). By varying the magnetic balance of the configuration, and the direction of the $\mathbf{B}\times\nabla\mathbf{B}$ ion drift in these plasmas the effect of operating in open and closed divertor geometry was examined [9]. Operational parameters included the toroidal field strength of 2.0 T, plasma current 1.3 MA, neutral beam heating power 5.5 MW, and a high-triangularity magnetic shape, of δ~0.75. The gap between the inner separatrix and the inner wall was 8.5 cm. Careful preparation of the vessel walls using helium glow discharge cleaning provided the sole means of pumping. Between these discharges, the pedestal density as the primary experimental parameter was matched to within 10%.

Operating in plasmas with the ion $\mathbf{B}\times\nabla\mathbf{B}$ drift direction into the upper divertor, tomographic reconstruction of image data from the divertor cameras, time-averaged over as much as 500 ms, produced a peak in D_α emissivity at the center post in the upper divertor for upper single-null plasmas, and in the lower divertor for lower single-null plasmas (Fig. 3).

The D_α emission was approximately two orders of magnitude higher in the divertor with the primary X-point. In balanced double-null with the same ion drift direction relative to the primary divertor, the D_α emission was symmetric at the inner and outer strike zones of each divertor, and the magnitude of emission in the lower divertor was about two orders of magnitudes higher than in the upper divertor. For the same set of plasmas, Abel inversion of the D_α emission profiles in the inner main SOL shows the emission to peak in the region closest to the divertor X-points (Fig. 3). In the double-null configuration the emission from the inner main SOL near the lower X-point was about twice as high as near the upper

X-point. Relative to the divertor, the peak D_α emission from the inner SOL was typically three orders of magnitude smaller. Analysis of the CII and CIII emission profiles, including modeling, are part of the ongoing effort and will be presented at a later time.

With increasing plasma density and heating power reflection of light at the lower baffle plate and port edges occurred, which complicated the analysis of the inner main SOL profiles. A comprehensive model of the vessel geometry and expected light sources is needed to account for these reflections. Local recycling of plasma at protruding surfaces, such as antenna guard and bumper limiters, which occur, as recently reported from JET [10], in particular during ELMs, will be assessed in future analysis.

This work was supported by the U.S. Department of Energy under Contracts W-7405-ENG-48 (LLNL) and DE-AC03-99ER54463 (DIII-D). The authors specially thank W.H. Meyer (LLNL) for providing computational support for the tomographic reconstruction algorithms. Contributions from A.W. Hyatt, T.C. Jernigan, J.A. Boedo, C.J. Lasnier, A.G. McLean, R.A. Moyer, D.L. Rudakov, P.C Stangeby, G. Wang, J.G. Watkins, and D.G. Whyte were greatly appreciated.

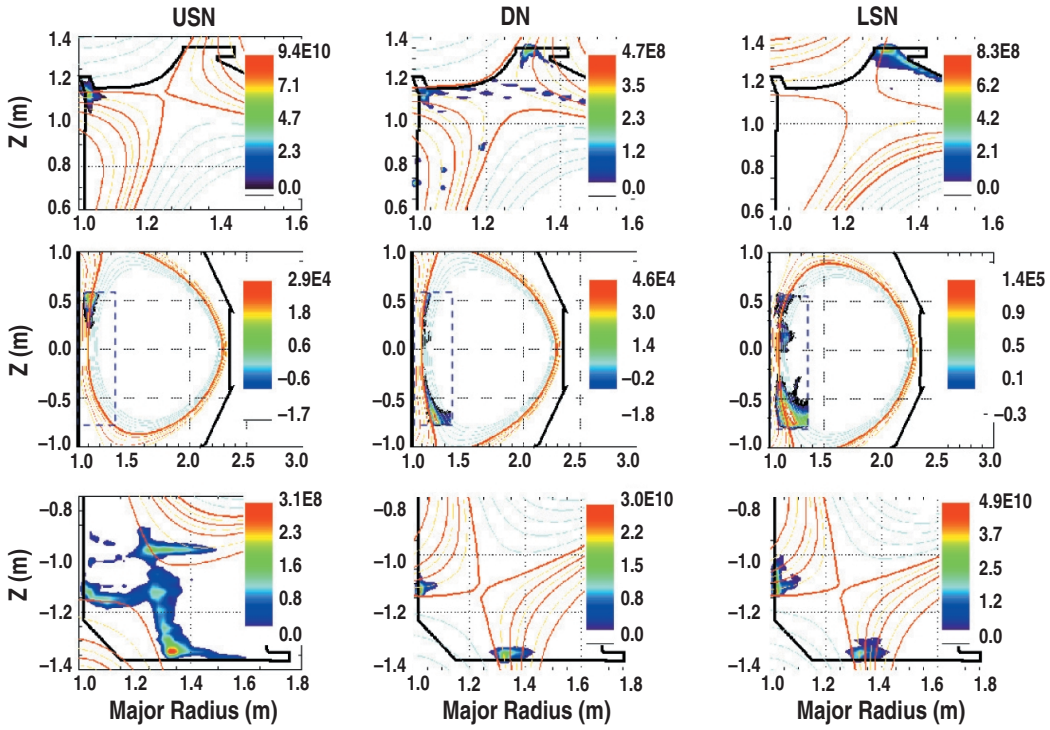

Fig. 3. Tomographically reconstructed and Abel-inverted D_α emission profiles in low-density, ELMy H-mode discharges (**B×∇B** ion drift into upper divertor). From left to right: upper single-null, balanced double-null, and lower single-null. From top to bottom: reconstruction of image data from the upper divertor, midplane, and lower divertor camera. For the midplane camera the rectangle visualizes the area which emission profiles were obtained by using an Abel inversion. Between the divertor cameras the calculated emissivities are relative, thus can be mutually compared. Emission profiles from midplane camera are currently uncalibrated.

[1] LaBombard, B., *et al*., Nucl. Fusion **40**, 2041 (2000).
[2] McCormick, K., *et al*., in Controlled Fusion and Plasma Physics (Proc. 20th Euro. Conf. Lisbon, 1993), Vol. **17C** (European Physical Society, Geneva, 1993) p. 597.
[3] Fenstermacher, M.E., *et.al*., Phys. Plasma **4**, 1761 (1997).
[4] Groth, M., *et al*., Rev. Sci. Instrum. **74**, 2064 (2003).
[5] Stangeby, P.C., *et al*., J. Nucl. Mater. **313-316**, 883 (2003).
[6] Rognlien, T.D., *et al*., J. Nucl. Mater. **196-198**, 347 (1992).

[7] Davis, J.W., and Haasz, A.A., J. Nucl. Mater. **241-243**, 347 (1997).
[8] Eckstein, W., *et al*., J. Nucl. Mater. **248**, 1 (1997).
[9] Petrie, T.W., *et al*., J. Nucl. Mater. **313-316**, 839 (2003).
[10] Ghendrih, Ph., *et al*., J. Nucl. Mater. **313-316**, 914 (2003).